Available online at www.sciencedirect.com
SCIENCE DIRECT
Journal of Photochemistry and Photobiology A: Chemistry 172 (2005) 126–134
Journal of Photochemistry and Photobiology A:Chemistry
www.elsevier.com/locate/jphotochem

Theoretical investigation on the one- and two-photon absorption properties of a series of porphyrazines with annulated 1,2,5-thiadiazole and 1,4-dimethyloxybenzene moieties

Xin Zhou[a], Ai-Min Ren[a], Ji-Kang Feng[a,b,*], Zhigang Shuai[c]

[a] *State Key Laboratory of Theoretical and Computational Chemistry, Institute of Theoretical Chemistry, Jilin University, Changchun 130023, China*
[b] *College of Chemistry, Jilin University, Changchun 130023, China*
[c] *The Center for Molecular Science, Institute of Chemistry, Chinese Academy of Sciences, Beijing 100080, China*

Received 18 September 2004; received in revised form 7 November 2004; accepted 2 December 2004
Available online 21 January 2005

Abstract

On the basis of equilibrium geometries optimized by B3LYP/6-31G(d) method, the one-photon absorption properties of a series of substituted porphyrazines have been investigated theoretically using time-dependent density functional theory and the semiempirical ZINDO method, respectively. The comparisons with the available experimental data confirmed that the reliability of the ZINDO method in predicting the electronic absorption properties. According to the one-photon absorption properties obtained from the ZINDO method, two-photon absorption properties of molecules have been studied, using ZINDO and sum-over-states methods. The results have showed that the molecule with symmetrically substituted with electron donors exhibits the maximum two-photon absorption cross-section (up to 5276.8 GM) in all the studied molecules. The molecular centrosymmetry has a positive effect on the enhancement of the two-photon absorption cross-section. For the molecules with multi two-photon absorption peaks, the cross-section in the region from 750 to 860 nm is enhanced by one order of magnitude compared with that in the region from 1050 to 1200 nm.

Keywords: Porphyrazine; Two-photon absorption; ZINDO; Sum-over-states

1. Introduction

Porphyrazine derivatives have attracted considerable experimental and theoretical interest initially because of their easily controlled properties by varying the substituents and the molecular design and their importance for the preservation of life [1], more recently because of their interesting chemical and physical properties and potential technological applications [2–4]. Porphyrazines are molecules with highly delocalized electronic structure in which the four pyrrole moieties are linked each other by four aza bridges. Currently, the linear and non-linear optical properties of porphyrazine analogs are widely investigated in terms of the design, synthesis and characterization of molecular materials for molecular electronics, optoelectronics and photonics [5–7].

An attractive optical non-linearity under intensive research is the two-photon absorption (TPA) process, in which an atom or a molecule simultaneously absorbs two photons, which can have the same or different energies. Materials with large TPA cross-sections have been found to be useful for a variety of applications, such as three-dimensional microfabrication [8–10], ultra-high-density optical data storage [11], biological imaging [12], and the controlled release of biologically relevant species [13]. TPA in tetrapyrrolic molecules has potential applications for optical power limiting and for holographic data storage [14–16]. Moreover, because tetrapyrrolic dyes serve as active structural units in various natural processes, such as oxygen transport, photosynthesis and electron transfer in cytochromes, they uniquely

* Corresponding author. Tel.: +86 431 8499856; fax: +86 431 8945942.
E-mail addresses: kabinzx@hotmail.com (X. Zhou), jikangf@yahoo.com (J.-K. Feng).

1010-6030/$ – see front matter © 2004 Elsevier B.V. All rights reserved.
doi:10.1016/j.jphotochem.2004.12.011

suitable for various biomedical applications, including cancer treatment by photodynamic therapy [17].

However, only a few experimental observations of TPA properties in tetrapyrrolic molecules have been reported in the literatures so far. Wen et al. [18] measured the TPA cross-sections of metal tetrakis-(3,4,5-trimethoxyphenyl)porphyrin) including chlorogallium(III), chloroindium(III), chlorothallium(III), tin(II) and lead(II) as central metal ions with the linear polarized nanosecond laser pulses at different wavelengths by Z-scan. The TPA cross-sections are in the range from 25 to 114 GM (where $1\,\mathrm{GM} = 1 \times 10^{-50}\,\mathrm{cm}^4\,\mathrm{s/photon}$). Rebane and co-workers [19] obtained the absolute TPA cross-sections for a series of porphyrins and tetrazaporphyrins with 100 fs duration pulses in two ranges of laser wavelengths, from 1000 to 1500 and from 700 to 800 nm. They found that the TPA cross-section in the Soret transition region is larger than that in the Q transition region by one order of magnitude. The tetrazaporphyrin symmetrically substituted with strong electron acceptors possesses the largest TPA cross-section—1600 GM. In contrast to the experimental investigations, there is only one theoretical report on the TPA properties of porphyrins. Birge and co-workers [20] studied the TPA properties of free base porphyrin, porphyrin dianion and the 2,4-substituted diformal and divinyl analogs of these molecules using a semiempirical SCF–MO formalism. They showed that a number of the two-photon allowed states in the Soret region are predicted to have TPA exceeding 100 GM.

In this paper, we theoretically investigated the one-photon absorption (OPA) properties of a series of porphyrazines with annulated electron-deficient 1,2,5-thiadiazole and the electron-donating 1,4-dimethyloxybenzene moieties, which were quite recently synthesized by Stuzhin and co-workers [21], by means of time-dependent density functional theory (TDDFT) and ZINDO, and then compared the results obtained from two methods with the experimental values. Then, ZINDO and sum-over-states (SOS) were employed to calculate the second hyperpolarizability and TPA properties of six molecules on the basis of geometries optimized by B3LYP/6-31G(d) and the OPA properties obtained from the ZINDO method.

2. Theoretical methodology

The structures of all porphyrazines have been predicted using the Kohn–Sham density functional theory (DFT) with the 6-31G(d) basis set. DFT calculations have been carried out using Becke's three-parameter hybrid functional [22,23], hereafter referred to as B3LYP. Time-dependent density functional theory [24] has been implemented in several quantum chemistry packages [24,25]. The vertical excitation energy and oscillator strength calculations were carried out using TDDFT with the same basis set and effective core potentials as those used in the ground-state DFT calculations at the B3LYP structures, as implemented in the GAUSSIAN 03 program.

The TPA process corresponds to simultaneous absorption of two photons. The TPA efficiency of an organic molecule, at optical frequency $\omega/2\pi$, can be characterized by the TPA cross-section $\delta(\omega)$. It can be directly related to the imaginary part of the second hyperpolarizability $\gamma(-\omega; \omega, \omega, -\omega)$ by [26,27]:

$$\delta(\omega) = \frac{3\hbar\omega^2}{2n^2c^2\varepsilon_0} L^4 \mathrm{Im}[\gamma(-\omega;\omega,-\omega,\omega)] \tag{1}$$

where $\hbar\omega$ is the energy of the incoming photons and ε_0 the vacuum electric permittivity. Here, n denotes the refractive index of the medium and L corresponds to the local-field factor. In the calculations presented here, these two quantities are set to 1 (isolated molecule in vacuum).

To compare the calculated TPA cross-section value with the experimental value measured in solution, the orientationally averaged (isotropic) value of γ is evaluated, which is defined as:

$$\langle\gamma\rangle = \frac{1}{15}\sum_{i,j}(\gamma_{iijj} + \gamma_{ijij} + \gamma_{ijji}), \qquad i, j = x, y, z \tag{2}$$

whereafter $\langle\gamma\rangle$ is shortened to γ and taken into the Eq. (1), and then the TPA cross-section is obtained.

The SOS expression to evaluate the components of the second hyperpolarizability $\gamma_{\alpha\beta\gamma\delta}$ can be induced out using perturbation theory and density–matrix method. By considering a power expansion of the energy with respect to the applied field, the $\gamma_{\alpha\beta\gamma\delta}$ Cartesian components are given by [28,29]:

$$\begin{aligned}
&\gamma_{\alpha\beta\gamma\delta}(-\omega_\sigma;\omega_1,\omega_{2,}\omega_3)\\
&= \hbar^{-3}\sum P_{1,2,3}\left(\sum_K{}'\sum_L{}'\sum_M{}'\left(\frac{\langle 0|\mu_\alpha|K\rangle\langle K|\overline{\mu_\beta}|L\rangle\langle L|\overline{\mu_\gamma}M\rangle\langle M|\mu_\delta|0\rangle}{(\omega_K - i\Gamma_K/2 - \omega_\sigma)(\omega_L - i\Gamma_L/2 - \omega_2 - \omega_3)(\omega_M - i\Gamma_M/2 - \omega_3)}\right.\right.\\
&\quad + \frac{\langle 0|\mu_\beta|K\rangle\langle K|\overline{\mu_\alpha}|L\rangle\langle L|\overline{\mu_\gamma}|M\rangle\langle M|\mu_\delta|0\rangle}{(\omega_K + i\Gamma_K/2 + \omega_1)(\omega_L - i\Gamma_L/2 - \omega_2 - \omega_3)(\omega_M - i\Gamma_M/2 - \omega_3)}\\
&\quad + \frac{\langle 0|\mu_\beta|K\rangle\langle K|\overline{\mu_\gamma}|L\rangle\langle L|\overline{\mu_\alpha}|M\rangle\langle M|\mu_\delta|0\rangle}{(\omega_K + i\Gamma_K/2 + \omega_1)(\omega_L + i\Gamma_L/2 + \omega_1 + \omega_2)(\omega_M - i\Gamma_M/2 - \omega_3)}\\
&\quad \left.\left. + \frac{\langle 0|\mu_\beta|K\rangle\langle K|\overline{\mu_\gamma}|L\rangle\langle L|\overline{\mu_\delta}|M\rangle\langle M|\mu_\alpha|0\rangle}{(\omega_K + i\Gamma_K/2 + \omega_1)(\omega_L + i\Gamma_L/2 + \omega_1 + \omega_2)(\omega_M + i\Gamma_M/2 + \omega_\sigma)}\right)\right)
\end{aligned}$$

$$-\sum_{K}{}'\sum_{L}{}'\left(\frac{\langle 0|\mu_\alpha|K\rangle\langle K|\mu_\beta|0\rangle\langle 0|\mu_\gamma|L\rangle\langle L|\mu_\delta|0\rangle}{(\omega_K - i\Gamma_K/2 - \omega_\sigma)(\omega_K - i\Gamma_K/2 - \omega_1)(\omega_L - i\Gamma_L/2 - \omega_3)}\right.$$
$$+\frac{\langle 0|\mu_\alpha|K\rangle\langle K|\mu_\beta|0\rangle\langle 0|\mu_\gamma|L\rangle\langle L|\mu_\delta|0\rangle}{(\omega_K - i\Gamma_K/2 - \omega_1)(\omega_L + i\Gamma_L/2 + \omega_2)(\omega_L - i\Gamma_L/2 - \omega_3)}$$
$$+\frac{\langle 0|\mu_\beta|K\rangle\langle K|\mu_\alpha|0\rangle\langle 0|\mu_\gamma|L\rangle\langle L|\mu_\delta|0\rangle}{(\omega_K + i\Gamma_K/2 + \omega_1)(\omega_K + i\Gamma_K/2 + \omega_\sigma)(\omega_L + i\Gamma_L/2 + \omega_2)}$$
$$\left.+\frac{\langle 0|\mu_\beta|K\rangle\langle K|\mu_\alpha|0\rangle\langle 0|\mu_\gamma|L\rangle\langle L|\mu_\delta|0\rangle}{(\omega_K + i\Gamma_K/2 + \omega_1)(\omega_L + i\Gamma_L/2 + \omega_2)(\omega_L - i\Gamma_L/2 - \omega_3)}\right)\Bigg) \qquad (3)$$

In this formula, α, β, γ and δ refer to the molecular axes, ω_1, ω_2 and ω_3 the optical frequencies and $\omega_\sigma = \omega_1 + \omega_2 + \omega_3$ the polarization response frequency, $\sum P_{1,2,3}$ a sum over the terms obtained by the six permutations of the pairs (ω_1/μ_β), (ω_2/μ_γ) and (ω_3/μ_δ), $|K\rangle$ an electronic wavefunction with energy $\hbar\omega_K$ relative to the ground electronic state, $\overline{\mu_s} = \mu_s - \langle 0|\mu_s|0\rangle$ the fluctuation dipole moment operator and μ_s is the dipole moment operator in the ξ Cartesian direction; the primes on the summation over the electronic states indicate exclusion of the ground state. In the present work, all damping factors Γ_s are set to 0.14 eV; this choice of damping factor is consistent with the width of the TPA spectra in a number of conjugated molecules and provides TPA cross-sections in good agreement with experimental data for a number of conjugated molecules [30].

3. Results and discussions

3.1. Molecular geometries and electronic structures

The molecular structures are chosen according to Fig. 1. They are a series of porphyrazines that bear peripheral annulated 1,2,5-thiadiazole and 1,4-dimethyloxy benzene rings, named **S4**, **S3A**, **S2A2**, **SASA**, **SA3** and **A4**, respectively (**A** symbolizes the annulated 1,4-dimethyloxybenzene ring and **S** is the 1,2,5-thiadiazole group in the pertinent fragments of porphyrazine macrocycle). The initial symmetry constraints are D_{2h} for **S4**, **SASA** and **A4**, C_{2v} for **S3A** and **SA3**, and there is no symmetric constraint on **S2A2**. Optimized results show that **A4** only has C_{2h} symmetry, in which C_2 axis goes through two H–N bonds. The symmetries of other molecules maintain. These six molecules

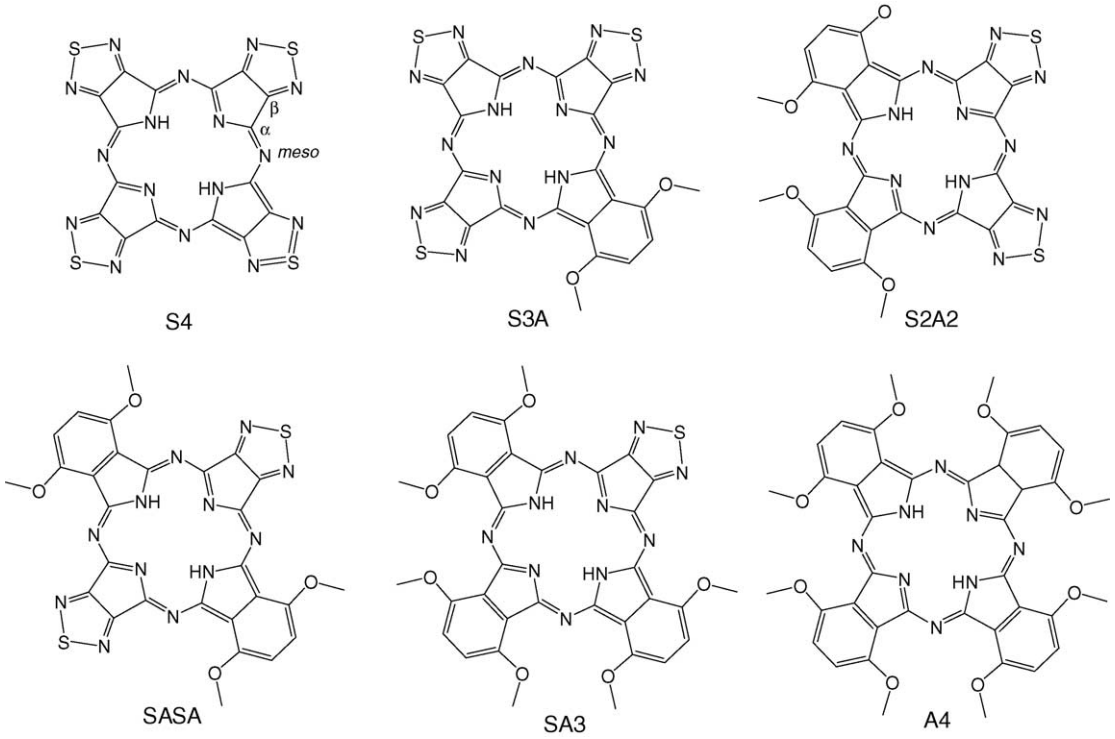

Fig. 1. Molecular structures and labels for the compounds studied.

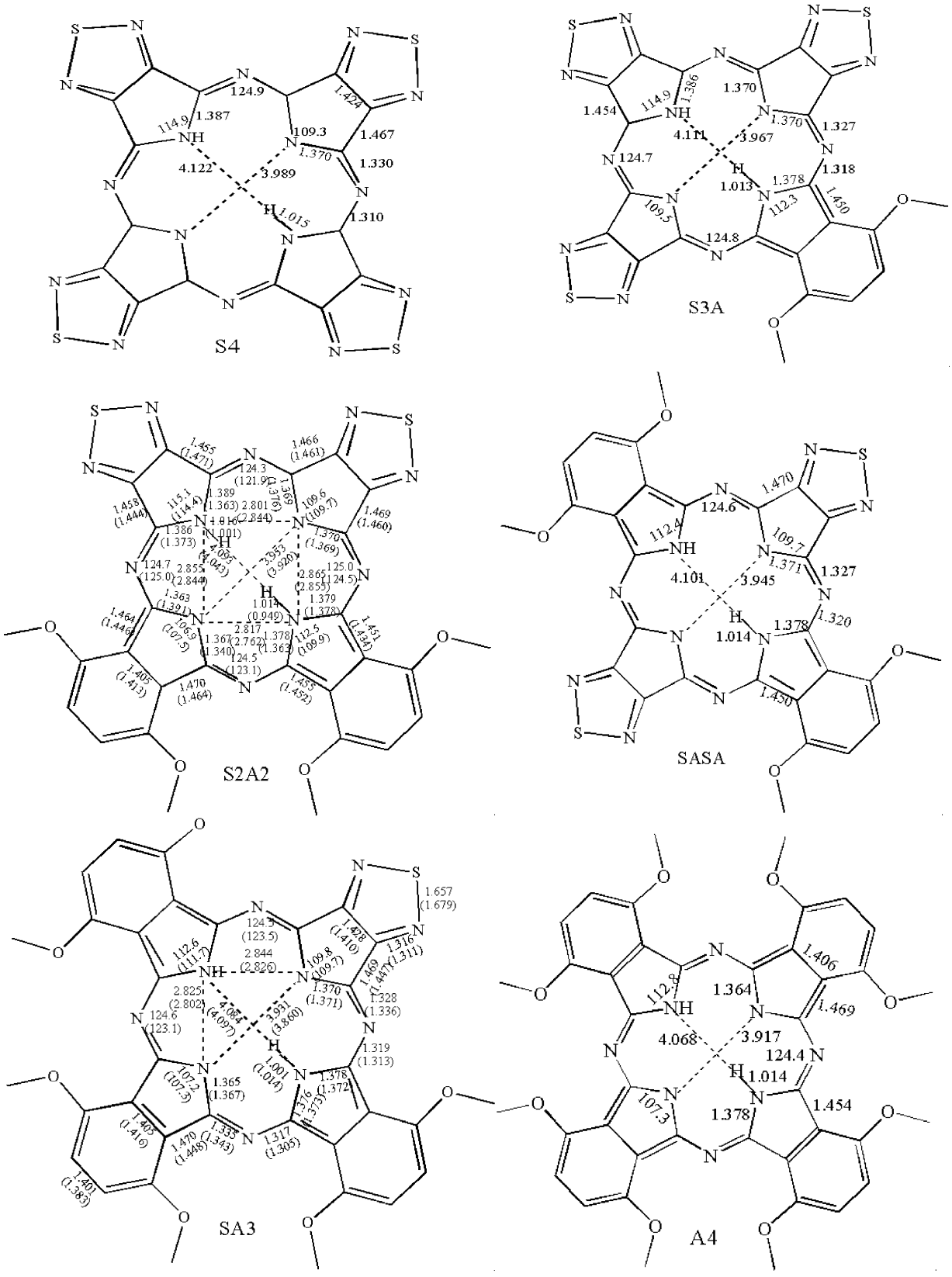

Fig. 2. Bond lengths and distance between the opposite atoms in the center in angstrom and bond angles in degree.

have perfect planarity except the peripheral methyloxy substituents.

Since the accuracy of the computed spectra is dependent upon the structural parameters used in the calculations, it is important to establish the quality of the calculated structures by comparing them with available experimental data. The calculated and observed geometrical parameters for the ground state of the some porphyrazines are displayed in Fig. 2. For **S2A2** and **SA3**, the X-ray data [21] are given in parentheses. It is seen that the predicted bond distances are slightly longer than those obtained from the crystal structure. The C–C and C–N distances are well within 0.02 Å of the observed values. The calculated bond angles are with 2.5° in experiment. These errors come from three reasons: (1) the structures in vacuum are more incompact than the crystal structures; (2) diamyloxybenzene rings in the experimental molecules are replaced by dimethyloxybenzene groups in the calculation; (3) the choice of the calculation method and the basis set is not perfect. Inspecting Fig. 2, we note that as dimethyloxy-subtituted benzene rings continuously replace thiadiazole rings (from **S4** to **A4**), the size of the central holes gradually processing from 4.122×3.989 Å^2 (for **S4**), to 4.111×3.967 Å^2 (for **S3A**), to 4.093×3.953 Å^2 (for **S2A2**) $\approx 4.101 \times 3.945$ Å^2 (for **SASA**), to 4.084×3.931 Å^2 (for **SA3**), to 4.068×3.917 Å^2 (for **S4**). The reduction in the central hole can be attributed to the fact that the dimethyloxybenzene ring annulated to the central tetrapyrrolic macrocycle is in favor of the charge transfer from the periphery to the center so that the whole molecule becomes more compact and the central hole becomes smaller.

Electronic structures are fundamental to the interpretation and understanding of the absorption spectra. The standard interpretation of the origin of the Q and B bands in the electronic absorption spectra of porphyrins, is based on the four-level model of Goutermans [31], which assumes that the HOMO and HOMO-1 are almost degenerate in energy and well separated from the other levels and a similar assumption is made for the LUMO and LUMO + 1. The symmetries and energies of the frontier orbitals for prophyrazines are listed in Table 1. From Table 1, one can find the assumption for LUMOs are basically presented in the studied porphyrazines. However, a large separation between the two highest occupied levels results in the fact that the four-level model no longer holds for these molecules. Fig. 3 displays the HOMO, LUMO and LUMO + 1 for every porphyrazine calculated by DFT method. The HOMOs are largely localized on C_α and phenyl rings. With the increase in the benzene rings, the delocation range of the whole molecule is enhanced. The LUMO and LUMO + 1 for porphyrazines receive a major contribution from the *meso*-N, C_α, C_β and pyrrole nitrogen atoms. Annulations of the methyloxy-substituted benzene rings in place of the 1,2,5-thidiazole rings lead to the destabilization of the HOMO and LUMO. The energy gap between HOMO and LUMO is gradually reduced as thiadiazole rings are replaced by methyloxybenzene rings one by one.

3.2. One-photon absorption

On the basis of the geometries optimized by B3LYP/6-31G(d), we have studied the OPA properties for all molecules. First, we will discuss the calculated OPA spectra of substituted porphyrazines by the TDDFT method. Computed vertical excitation energies and oscillator strengths of molecules are summarized in Table 2 with the experimental data available [21]. As shown in Table 2, TDDFT calculations do not reproduce completely the experimentally red-shift trend. This deviation originates from defects of TDDFT method [32]. We can find the Q band peaks obtained by TDDFT method are smaller than the experimental values by about 50–100 nm. The TDDFT calculations significantly underestimate the Q

Table 1
Calculated orbital energies (eV) and symmetries by DFT method

S4		**S3A**		**S2A2**		**SASA**		**SA3**		**A4**	
Symmetry	Energy	Symmetry	Energy	Symmetry	Energy	Symmetry	Energy	Symmetry	Energy	Symmetry	Energy
Virtual orbitals											
b_{3g}	−0.64	b_2	−0.29	a_1	0.04	b_{1g}	0.10	b_2	0.35	a_u	1.10
a_u	−1.48	b_1	−0.54	a_1	−0.05	b_{2g}	−0.03	b_1	0.29	a_u	0.59
b_{1g}	−2.23	a_2	−1.24	a_1	−0.31	b_{1u}	−0.36	a_2	0.14	b_g	0.49
b_{3u}	−2.39	a_2	−1.91	a_1	−1.01	a_u	−1.03	b_1	−0.15	b_g	0.31
b_{2g}	−2.44	b_1	−2.05	a_1	−1.65	b_{3g}	−1.63	a_2	−0.84	a_u	0.04
b_{3u}	−2.87	b_1	−2.29	a_1	−1.97	b_{1u}	−1.80	b_1	−1.43	a_u	−0.67
b_{1g}	−3.73	a_2	−3.32	a_1	−2.87	b_{2g}	−2.83	a_2	−2.53	b_g	−2.19
b_{2g}	−3.97	b_1	−3.41	a_1	−3.04	b_{3g}	−2.96	b_1	−2.57	b_g	−2.24
Occupied orbitals											
a_u	−6.10	a_2	−5.44	a_1	−4.94	a_u	−4.93	a_2	−4.54	a_u	−4.18
b_{3u}	−7.60	a_2	−6.38	a_1	−5.75	b_{3g}	−5.81	a_2	−5.48	b_g	−5.23
b_{1g}	−7.66	a_1	−7.16	a_1	−6.20	a_u	−6.23	b_1	−5.58	a_u	−5.26
b_{3u}	−7.91	a_2	−7.32	a_1	−6.65	b_{1u}	−6.72	a_2	−6.07	b_g	−5.37
b_{3g}	−8.02	a_2	−7.43	a_1	−6.86	b_{1g}	−6.96	b_1	−6.30	a_u	−5.93
b_{2u}	−8.16	a_1	−7.47	a_1	−6.93	b_{3g}	−7.01	b_2	−6.53	a_u	−5.94
b_{2g}	−8.24	a_1	−7.62	a_1	−7.08	b_{1u}	−7.14	b_1	−6.54	b_g	−6.15
b_{3u}	−8.29	a_2	−7.71	a_1	−7.27	b_{2g}	−7.21	b_1	−6.79	b_g	−.615

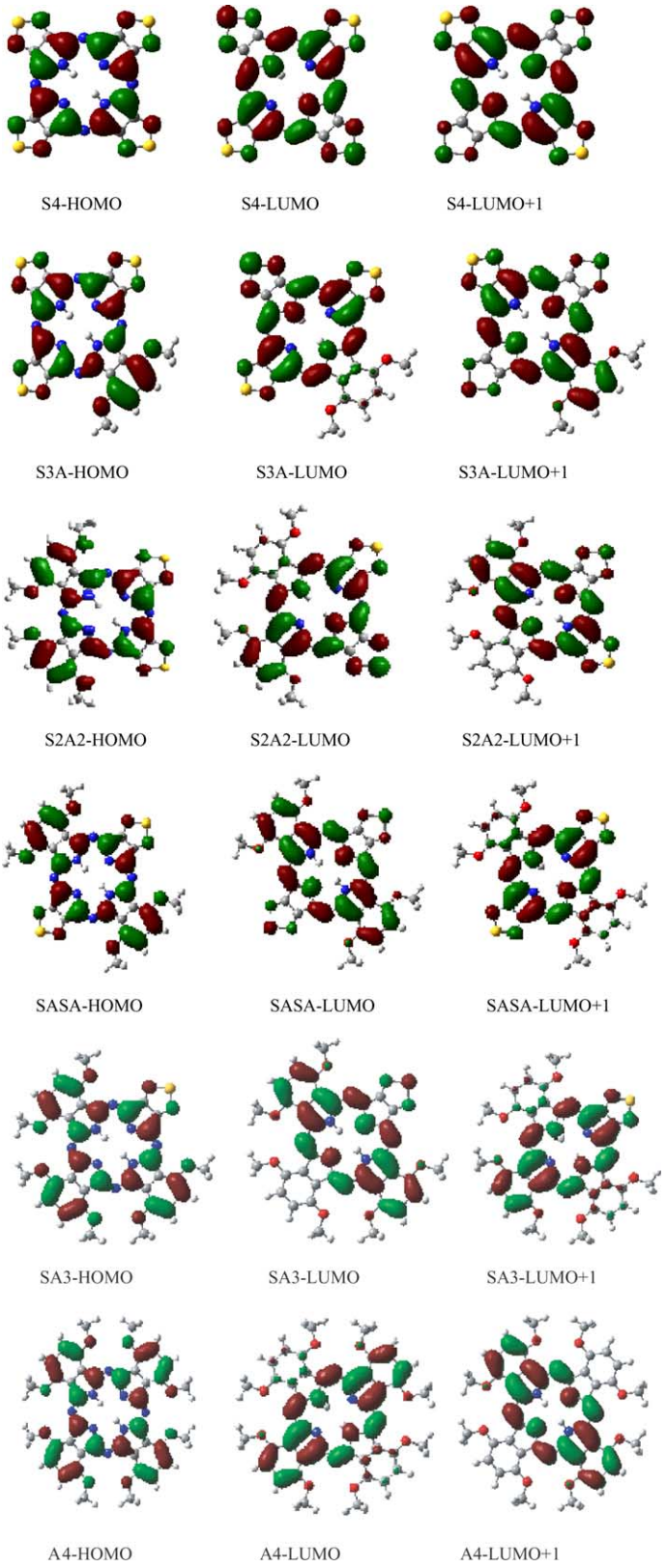

Fig. 3. HOMO and LUMOs orbitals for the porphyraines.

Table 2
Calculated one-photon absorption parameters by TDDFT and ZINDO and the corresponding experimental values

TDDFT λ (nm)	ZINDO λ (nm)	Experimental (nm) [21] λ
S4		
605.2 (0.28)	717.3 (0.21)	649
569.7 (0.23)	671.8 (0.33)	
328.3 (1.10)	319.1 (1.59)	332
305.4 (0.97)		
S2A2		
682.3 (0.58)	745.1 (0.31)	735
633.3 (0.25)		
325.9 (0.49)	329.8 (0.29)	336
302.3 (0.64)		
S3A		
677.5 (0.16)	699.1 (0.41)	715
626.4 (0.43)		
334.3 (0.58)	311.2 (0.66)	335
309.8 (0.61)		
SA3		
677.6 (0.45)	752.6 (0.52)	766
657.2 (0.33)		
319.6 (0.82)	329.8 (0.54)	329
SASA		
668.0 (0.58)	738.3 (0.52)	724
654.5 (0.18)		
321.2 (0.70)	304.5 (1.01)	333
318.7 (0.87)		
A4		
674.5 (0.42)	755.1 (0.62)	769
670.3 (0.50)	704.9 (0.69)	
319.9 (0.99)	343.6 (0.52)	330
318.4 (0.83)	329.8 (0.34)	
	311.4 (0.53)	

Note: Oscillator strength is given in parentheses.

band absorptions with the average error equal to 8.8%. The TDDFT Soret peaks are in good agreement with the experimental data with the errors being 2%. Second, we analyze the calculated OPA properties obtained by the ZINDO method. The ZINDO calculations employed here includes single excitations between 14 occupied orbitals and 14 unoccupied orbitals, and double excitations among the 3 highest occupied and 4 lowest unoccupied molecular orbitals, in all the summation is performed over 293 excited states including the ground state. As shown in Table 2, the Q band absorption peaks of all six compounds predicted by the ZINDO method are in better agreement with the experimental observations than that of TDDFT calculations, with the average deviations in 3% from the experimental data. For example, for **SASA**, the ZINDO result is 738.3 nm, which is longer than the TDDFT result (668.0 nm) and close to the experimental value (724 nm) taken from the literature [32]. As the case of the B band absorption obtained by the ZINDO method, the average error in the calculations is 4%. It is notable that the ZINDO calculations successfully reproduce the red-shift of Q bands in the experiment observation. In gen-

eral, from the view of the reproduction of the experimental trend and the simulation of the whole spectrum of every compound, the semi-empirical ZINDO method exhibits more reliable results than TDDFT for this series of porphyrazines.

3.3. Two-photon absorption

According to Eqs. (1)–(3), we compiled a program to calculate the orientational average second hyperpolarizability $\langle\gamma\rangle$ and TPA cross-section $\delta(\omega)$. The TPA spectra calculated

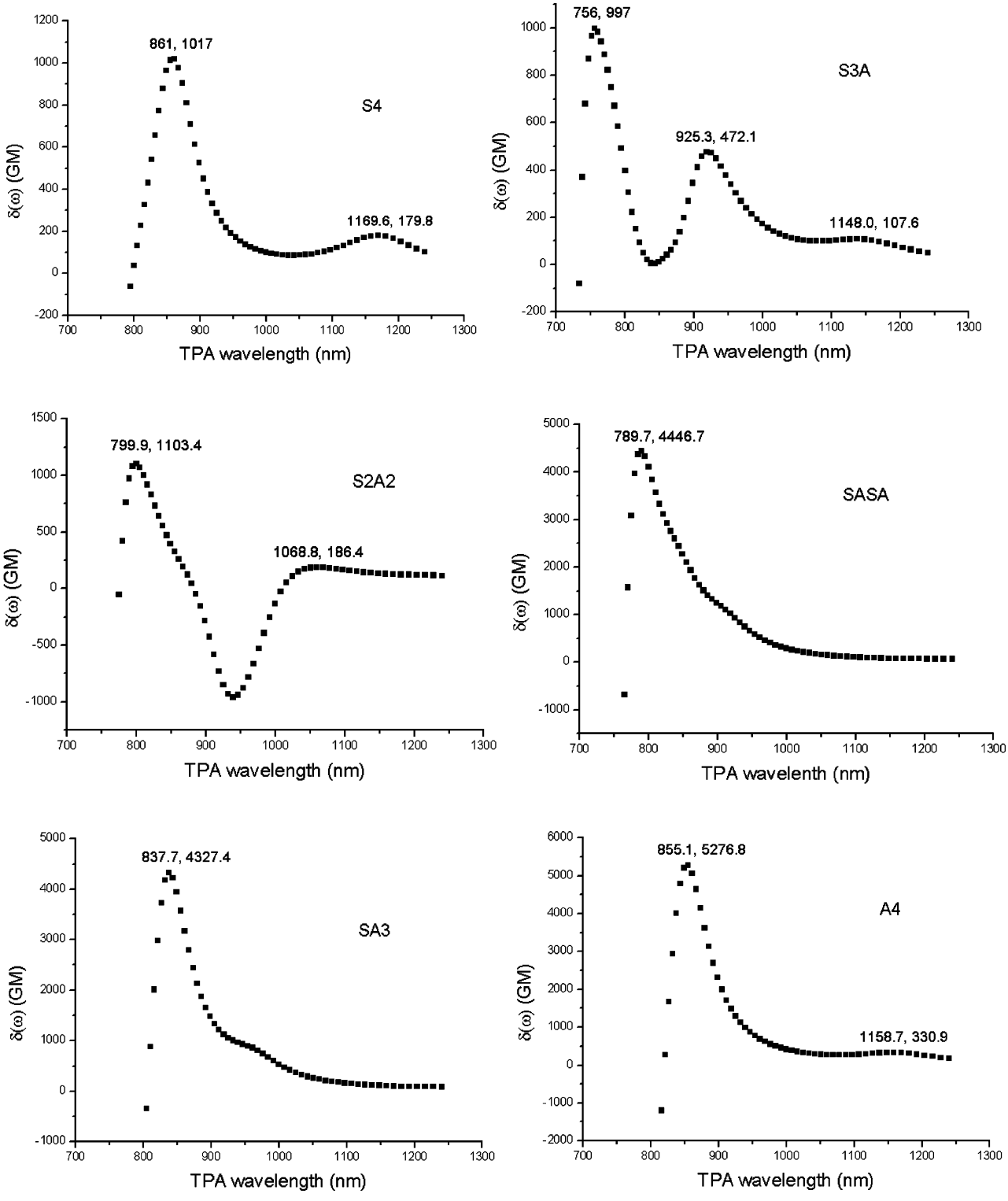

Fig. 4. Two-photon absorption spectra of studied molecules.

Table 3
Two-photon absorption properties for porphyrazines

Molecule	$(\lambda_{max})^2$ (nm)	δ_{max} (GM)
S4	861.0	1017.7
	1169.6	179.8
S3A	756.0	997.2
	925.3	472.1
	1148.0	107.6
S2A2	799.9	1103.4
	1068.8	186.4
SASA	789.7	4446.7
SA3	837.7	4327.4
A4	855.1	5276.8
	1158.7	330.9

by the method above are shown in Fig. 4. The calculated TPA properties of six molecules are listed in Table 3. In many applications of two-photon features, molecules with very large TPA cross-sections are required in a range of fundamental excitation wavelengths in the range of 600–1200 nm. From Table 3 and Fig. 4, one can see the TPA peak wavelengths range from 700–1200 nm, all sitting in infrared, and the magnitude of TPA cross-sections is 100–5000 GM. This indicates they satisfy the requirements of application using two-photon properties. For molecules with different structures, the TPA spectra are distinct. For **S4**, there are two TPA peaks in the spectrum of Fig. 4. The first weaker peak appears at 1169.8 nm and the TPA cross-section is 179.8 GM. The second maximum TPA cross-section is 1017.7 GM at 861.0 nm. Processing from **S4** to **S3A**, the third peak is observed at 925.3 nm and the corresponding TPA cross-section is equal to 472.1 GM. Other two peaks are blue-shifted compared with that of **S4** (from 861.0 to 756.0 nm and from 1169.6 to 1148.0 nm) and the relative TPA cross-section maxima are decreased from 1017.7 to 997.2 GM and from 179.8 to 107.6 GM. These differences partly come from the reduction in molecular point symmetry from D_{2h} for **S4** to C_{2v} for **S3A**. From **S3A** with C_{2v} symmetry to **S2A2** with C_1 symmetry, the peak at ∼900 nm has disappeared and other two peaks maintain. Two absorption maxima of **S2A2** are observed at 1068.8 nm and 799.9 nm, which are red-shifted on the basis of that for **S3A**. The maximum TPA cross-section values of **S3A** are slight larger than that of **S2A2**. As the case of **SASA** (the isomer of **S2A2**), the TPA cross-section is found to be around 4446.7 GM at 789.7 nm, which is larger than that of **S2A2** by about four times. This obvious difference results from the different positions of dimethyloxybenzene rings. In this series of porphyrazines, the central porphyrazine ring with 18π-electrons is regarded as the electron acceptor. For **SASA**, the dimethyloxybenzene rings as electron donors are opposite to each other and the D–π–D structure is more favor to the charge-transfer from peripheral to the center than that for **S2A2**. The maximum TPA cross-section of **SA3** (4327.4 GM) is little smaller than that of **SASA** (4446.7 GM). This result partly roots in the reduction of molecular point symmetry from D_{2h} (**SASA**) to C_{2v} (**SA3**). In the six studied porphyrazines, **A4** with symmetrically substituted electron donors exhibits the maximum TPA cross-section values as 5276.8 GM at 855.1 nm. The position of the weaker peak is at 1158.7 nm and the corresponding TPA cross-section maxima is equal to 330.9 GM.

Analyzing the results above, we obtained the following conclusions:

(i) The opposite appearance of electron-donors (D–π–D structure) in the whole molecule has an overriding influence on the increase of the TPA cross-section values. The TPA cross-sections of **SASA**, **SA3** and **A4** are about four times as that of **S4**, **S3A** and **S2A2**.

(ii) The molecules with centrosymmetry, such as C_{2h} and D_{2h} exhibit larger TPA cross-sections than those without central symmetry $\delta_{S4(D_{2h})} > \delta_{S3A(C_{2v})}$, $\delta_{A4(C_{2h})}$ $\delta_{SASA(D_{2h})} > \delta_{SA3(C_{2v})}$. As far as porphyrazines presenting multi peaks are concerned, the TPA cross-sections in the region from 750 to 860 nm are enhanced by one order of magnitude on the basis of that in the region from 1050 to 1200 nm. The similar results are observed by Drobizhev and co-workers [19]. They measured the absolute TPA cross-section in two ranges of laser wavelengths, from 1100 to 1500 nm and from 700 to 800 nm. The experimental results showed that the cross-section in the Soret transition region is larger than that in the Q transition region by approximately one order of magnitude. It is obvious that our calculations are reasonable and can give some useful information of understanding molecular structure-properties relationships.

(iii) This series of symmetrical and unsymmetrical porphyrazines with annulated 1,2,5-thiadiazole and 1,4-dimethyloxybenzene moieties exhibit large TPA cross-sections as high as 1000–5000 GM. These values are orders of magnitude higher than commercially available organic dyes. So, they are promising TPA materials and worthy being investigated experimentally in the future.

4. Summary

We have studied theoretically the one- and two-photon absorption properties of a series of symmetrical and unsymmetrical porphyrazines. The calculated results are in good agreement with the experimental observations. The symmetrical substitution of electron-donors and the molecular centrosymmetry play the important roles in the enhancement of TPA cross-sections. The prediction of TPA cross-section shows this kind of porphyrazines possesses good TPA properties and may be promising TPA materials.

Acknowledgements

This work is supported by the National Nature Science Foundation of China (20273023, 90101026) and the Key Laboratory for Supramolecular Structure and Material of Jilin University.

References

[1] D. Dolphin (Ed.), The Porphyrins, Academic Press, New York, 1978–1979.
[2] R.W. Wagner, J.S. Lindsey, J. Seth, V. Palaniappan, D.F. Bocian, J. Am. Chem. Soc. 118 (1996) 3996.
[3] J.R. Reimers, T.X. Lü, M.J. Crossley, N.S. Hush, Chem. Phys. Lett. 256 (1996) 353.
[4] S. Belviso, G. Ricciardi, F. Lelj, J. Mater. Chem. 10 (2000) 297.
[5] S. Pryadarshy, M.J. Therien, D.N. Beratan, J. Am. Chem. Soc. 118 (1996) 1504.
[6] D. Beljonne, G.E. O'Keefe, P.J. Hamer, R.H. Friend, H.L. Anderson, J.L. Brédas, J. Chem. Phys. 106 (1997) 9439.
[7] Z. Wang, P.N. Day, R. Pachter, J. Chem. Phys. 108 (1998) 2504.
[8] S. Maruo, O. Nakamura, S. Kawata, Opt. Lett. 22 (1997) 132.
[9] S. Maruo, K. Ikuta, Proc. Soc. Photo-Opt. Instrum. Eng. 3937 (2000) 106.
[10] S. Kawata, H.-B. Sun, T. Tanaka, K. Takada, Nature 412 (2001) 697.
[11] H.E. Pudavar, M.P. Joshi, P.N. Prasad, B.A. Reinhardt, Appl. Phys. Lett. 74 (1999) 1338.
[12] W. Denk, Proc. Natl. Acad. Sci. U.S.A. 91 (1994) 6629.
[13] R.M. Williams, D.W. Piston, W.W. Webb, Fed. Am. Soc. Exp. Biol. J. 8 (1994) 804.
[14] M. Drobizhev, A. Karotki, A. Rebane, Chem. Phys. Lett. 334 (2000) 76.
[15] G.L. Wood, M.J. Miller, A.G. Mott, Opt. Lett. 20 (1995) 973.
[16] M. Drobizhev, C. Sigel, A. Rebane, J. Lumin. 86 (2000) 391.
[17] B.W. Henderson, T.J. Dougherty, Photochem. Photobiol. 55 (1992) 147.
[18] T.C. Wen, L.C. Hwang, W.Y. Lin, C.H. Chen, C.H. Wu, Chem. Phys. 286 (2002) 293.
[19] A. Karotki, M. Drobizhev, M. Kruk, C. Spangler, E. Nickel, N. Mamardashvili, A. Rebane, J. Opt. Soc. Am. B 20 (2003) 321.
[20] M.B. Masthay, L.A. Findsen, B.M. Pierce, D.F. Bocian, J.S. Lindsey, R.B. Birge, J. Chem. Phys. 84 (1986) 3901.
[21] M.P. Donzello, C. Ercolani, A.A. Gaberkorn, E.V. Kudrik, M. Meneghetti, G. Marcolongo, C. Rizzoli, P.A. Stuzhin, Chem. Eur. J. 9 (2003) 4009.
[22] A.D. Becke, Phys. Rev. A 38 (1988) 3098.
[23] C. Lee, W. Yang, R.G. Parr, Phys. Rev. B 37 (1988) 785.
[24] R.E. Stratmann, G.E. Scuseria, M.J. Frisch, J. Chem. Phys. 109 (1998) 8218.
[25] R. Bauernschmitt, R. Ahlrichs, Chem. Phys. Lett. 256 (1996) 454.
[26] M. Cha, W.E. Torruellas, G.I. Stegeman, W.H.G. Horsthuis, G.R. Möhlmann, J. Meth, Appl. Phys. Lett. 65 (1994) 2648.
[27] T. Kogej, D. Beljonne, F. Meyers, J.W. Perry, S.R. Marder, J.-L. Brédas, Chem. Phys. Lett. 298 (1998) 1.
[28] B.J. Orr, J.F. Ward, Mol. Phys. 20 (1971) 513.
[29] D.M. Bishop, J.M. Luis, B. Kirtman, J. Chem. Phys. 116 (2002) 9729.
[30] M. Albota, D. Beljonne, J.L. Brédas, J.E. Ehrlich, J. Fu, A.A. Heikal, S.E. Hess, T. Kogej, M.D. Levin, S.R. Marder, D. McCord-Maughon, J.W. Perry, H. Röckel, M. Rumi, G. Subramaniam, W.W. Webb, X. Wu, C. Xu, Science 281 (1998) 1653.
[31] M. Gouterman, J. Mol. Spectrosc. 6 (1961) 138.
[32] J. Ma, S. Li, Y. Jiang, Macromolecules 35 (2002) 1109.